

Thermal Stability and Dielectric Relaxation of Natural Rubber/Soda Lignin and Natural Rubber/Thiolignin Composites

S. H. Botros,¹ M. A. M. Eid,² Z. A. Nageeb³

¹Polymers Department, National Research Centre, Dokki, Cairo, Egypt

²Microwave Physics Department, National Research Centre, Dokki, Cairo, Egypt

³Cellulose and Papers Department, National Research Centre, Dokki, Cairo, Egypt

Received 16 September 2004; accepted 17 May 2005

DOI 10.1002/app.22865

Published online 16 December 2005 in Wiley InterScience (www.interscience.wiley.com).

ABSTRACT: The influence of soda lignin and thiolignin on the mechanical properties (tensile strength and elongation at rupture) as well as on the dielectric properties (conductivity (σ), permittivity (ϵ'), dielectric loss (ϵ''), and dielectric relaxation time (τ)) of their composites with natural rubber (NR) was investigated. All measurements were carried out on NR, NR/soda lignin (20 phr), and NR/thiolignin (20, 30, and 40 phr) composites. The mechanical properties reveal that NR/thiolignin composite possesses the best thermal stability and 20 phr is the optimum thiolignin loading. The dielectric study was carried out over a frequency range

from 100 Hz to 100 kHz at temperature range from 20 to 80°C. Dielectric data were fitted in the frequency domain using Havriliak-Negami and Fröhlich functions in addition to the conductivity term. The different relaxation mechanisms in the system were also discussed according to these functions. © 2005 Wiley Periodicals, Inc. *J Appl Polym Sci* 99: 2504–2511, 2006

Key words: natural rubber; soda lignin; thiolignin; dielectric relaxation; composites; mechanical properties

INTRODUCTION

Lignin, a renewable waste material of pulp and paper industries, was found to be structurally similar to kraft lignin. Surface modification by addition of benzoyl peroxide has caused generation of new functional groups in lignin. Efficacy of the crude lignin as well as that of the modified variety as a filler in nitrile rubber has been evaluated. Modified lignin has been found to produce superior elongation, hardness, and compression set properties when compared with phenolic resin but inferior to carbon black. Also, both thermogravimetric analysis and thermomechanical analysis showed highest thermal stability for the modified lignin.¹ Lignin or its derivatives can be used as specific filler to polymer composites. Its addition to rubber leads to increase of hardness and to improvement of abrasion, but it causes a decrease of mechanical properties, especially of tensile strength and modulus. The effect of methylated lignin, thiolignin, and lignosulfonate on physical and mechanical properties of lignin-filled styrene butadiene rubber has been investigated. It has been found that lignosulfonate decreased

the cure time and acted as secondary accelerator, while methylated lignin and thiolignin increased the crosslink density and could be used as reinforcing fillers.² Besides their use as filler, lignins in the form of low- to higher-molecular-weight, melt able or soluble products can be specially tailored for plastics and rubber compounding.³ Since, lignin is a three-dimensional polymer that basically consists of variously substituted phenylpropane units linked by aryl-aryl ether, aryl-alkyl ether, and carbon-carbon bonds. The reactivity of lignin depends mainly on aliphatic and phenolic hydroxyl groups as well as carbonyl groups. The basic skeletons and functional group contents of lignins depend on their sources and the chemical and the structural characteristics of lignins from a given source. Although numerous studies on lignin properties and its utilization have been conducted in the past two decades, commercial uses of technical lignins have been hindered by their inherent variability, molecular complexity, and low reactivity because of the condensation of potentially reactive groups.^{4–6}

Mechanical behavior of natural rubber (NR)-cellulose II composites has been investigated. The composite with 15 phr of Cel II was found to give the best tensile and tear performances.^{7,8} Also, the mechanical and electrical properties of NR vulcanizates loaded with lignocellulosic materials have been studied. It has been found that the stress of vulcanizates decreased with initial fiber loading. Also, the resistivity

Correspondence to: S. H. Botros (sh50_botros@hotmail.com).

ρ , dielectric permittivity ϵ' , and dielectric loss ϵ'' have been determined. It was noticed that $\epsilon \ll \rho$ for bagasse pulp was higher than that for cotton stalks pulp, which is attributed to the higher hemilignin content in bagasse pulp that is characterized with a low degree of polarization. Also, abrupt increase of ϵ' at higher bagasse pulp content was noticed.⁹

In the present work, NR/soda lignin and NR/thiolignin composites were prepared. Thermal stability of the composites obtained was evaluated with assessment of the physicochemical properties after and before accelerated thermal ageing. Also, the dielectric properties of the composites will be discussed.

EXPERIMENTAL

Materials

NR of the type smoked sheets, a product of Malaysia, was used in the present research. Hi-sil (hydrated silica), a product of Bayer Company (Leverkosen, Germany), was used as reinforcing filler for rubber vulcanizates. The other compounding rubber ingredients were of pure grade used in industry.

Synthesis of thiolignin

It was prepared with Kraft cooks method from the black liquor of the sulfate process of bagasse. The cooking was carried out at 160°C cooking temperature for 1 h. Alkali ratio was 20% based on dry weight of wood. Sulfidity was 25% and the liquor ratio was 5 : 1. Thiolignin was precipitated from concentrated liquor with dilute sulfuric acid. The colloidal lignin precipitate was coagulated with acetic anhydride,¹⁰ then filtered, washed, and vacuum-dried at 50°C.

Synthesis of soda lignin

It was prepared with soda pulping process, under the same conditions mentioned earlier for thiolignin, but without adding sodium sulfide.

Elemental analysis

The percentages of C, H, and S were determined with using normal combustion method, utilizing Elemental Analyzer, Perkins-Elmer, Elementar, Hanau, Germany. Oxygen was determined with difference method.

Methoxyl content

It was determined by a modified Zeisel-viebock method as given by Klimova et al.¹¹

Phenolic hydroxyl groups

They were determined with electronic spectra based on ultraviolet absorption of phenol in alkaline solution.

Infrared spectroscopy

The Infrared absorption spectra of the isolated lignin samples were determined using Beckman IR spectrophotometer 4220 utilizing potassium bromide discs. Isolated lignin samples were examined in clear discs containing 1.8 mg of lignin in 100 mg of potassium bromide.

Mixing, vulcanization, and testing of rubber

NR was mixed with curatives and other compounding ingredients on an open two roll mill of 170-mm diameter and 300-mm working distance. The rheometric characteristics¹² were assessed with a Monsanto Oscillating Disc Rheometer R-100 at (142 ± 1)°C. The blends were then cured in a hydraulic press at the same temperature. The physicochemical properties were determined with a Zwick-1425 tensile tester.¹³ Accelerated thermal ageing of rubber vulcanizates was carried out in an air-circulated electric oven at 90°C, according to standard method.¹⁴

Dielectric measurements

Dielectric measurements were carried out in the frequency range 100 Hz up to 100 kHz by using an LCR meter type AG-411 B (Ando electric Ltd., Japan). The capacitance (C) and the loss tangent (tan δ) were obtained directly from the bridge from which the permittivity (ϵ') and dielectric loss (ϵ'') were calculated. A guard ring capacitor of the type NFM/5T Wiss Tech. Werkstätten (WTW) GMBH, Germany, was used as a measuring cell. The cell was calibrated by using standard materials¹⁵ and the experimental error in ϵ' and ϵ'' was found to be ±3% and ±5%, respectively. The temperature of the cell was controlled to within ±0.1°C by circulation of water from an ultrathermostat through a jacket surrounding the cell.

RESULTS AND DISCUSSION

Elemental analysis

It is clear from Table I that phenolic OH/OCH₃ ratio in thiolignin for kraft cooks of bagasse is higher than that for soda cooks. Thus, the OH/OCH₃ ratio appears to be dependent on the method of cooking. However, the MeO content and the number of MeO/C₉ for soda lignin isolated from the black liquor of soda cooks are higher than those for thiolignin isolated from kraft cooks. On the other hand, thiolignin has higher OH/C₉ than those isolated from soda cooks.

TABLE I
Elemental Analysis and Functional Groups of Soda Lignin and Thiolignin

Type of lignin	Analysis (%)							No. of atoms and functional groups					
	C	H	O	S	OH	OCH ₃	OH/OCH ₃	C	H	O	S	OH	OCH ₃
Soda lignin	61.8	6.0	32.2	—	2.3	16.6	0.250	9	8.2	2.6	—	0.26	1.0
Thiolignin	63.8	5.7	26.2	4.4	3.5	14.4	0.443	9	7.6	1.8	0.25	0.38	0.86

Infrared spectrum

The infrared spectra of soda lignin extracted from soda cooking of bagasse and thiolignin obtained with kraft process are shown in Figures 1(a) and 1(b).

It is observed that all the bands of both soda lignin and thiolignin are nearly similar.^{16–18} The essential difference observed for the absorption in the region 600–700 cm⁻¹ is attributed to the C—S vibrations appeared in the spectrum of thiolignin. Very weak band at 630 cm⁻¹ in softwood thiolignin has been assigned to C—S stretching.¹⁹ In the region 600–700 cm⁻¹, no band appeared in the spectrum of soda lignin [Fig. 1(a)].

Mechanical properties

NR/soda lignin and NR/thiolignin composites

Soda lignin and thiolignin obtained were incorporated into NR mixes. Formulations and rheological proper-

ties of NR/soda lignin and NR/thiolignin composites are listed in Table II. It is obvious that the incorporation of either soda lignin or thiolignin into NR mixes results in increasing the maximum torque of the composites obtained. The great increase of maximum torque in case of thiolignin can be attributed to the sulfur present in thiolignin. Also, the incorporation of either soda lignin or thiolignin into NR mixes results in shorter cure times (tc₉₀) with higher rate indices. The physicomechanical properties of NR and its composites with either soda lignin or thiolignin were measured and illustrated in Figure 2. The tensile strengths of NR/soda lignin and NR/thiolignin composites are lower than that of the blank (NR) vulcanizate. However, elongations at break of the composites are slightly less than that of the blank vulcanizate.

The vulcanizates of NR and its composites with either soda lignin or thiolignin were then subjected to thermal

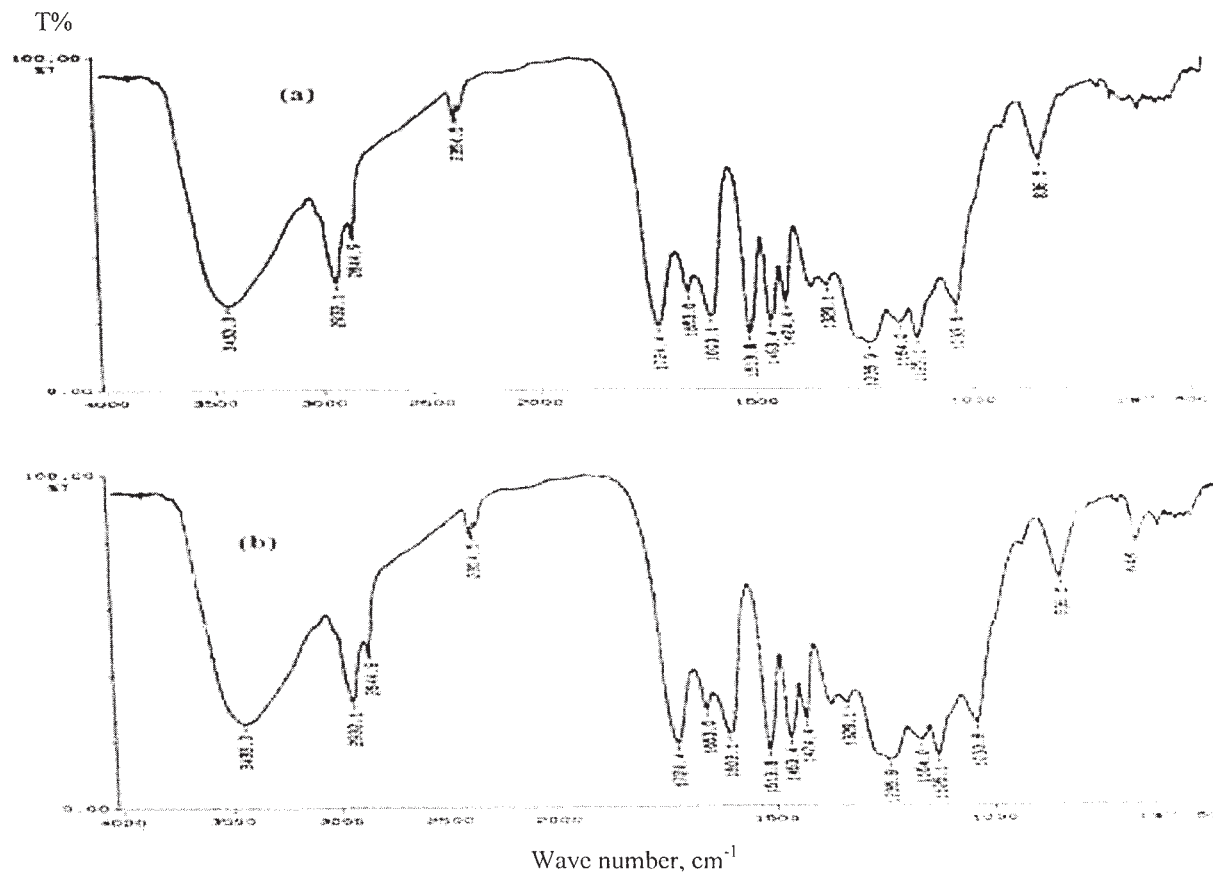


Figure 1 Infrared spectra of (a) soda lignin and (b) thiolignin.

TABLE II
Formulations and Rheological Properties of Natural Rubber Mixes with and Without Soda Lignin and Thiolignin

	S1	S2	S3	S4	S5
Ingredients (phr)					
NR	100	100	100	100	100
Zinc oxide	5	5	5	5	5
Stearic acid	2	2	2	2	2
Silica	20	20	20	20	20
Lignin	0	20	0	0	0
Thiolignin	0	0	20	30	40
Processing oil	5	5	5	5	5
CBS	1	1	1	1	1
Sulfur	2	2	2	2	2
Rheological properties					
Minimum torque (Nm)	4.5	3	7	5	5
Maximum torque (Nm)	49	52	64	60	62
Scorch time (ts2, min)	7.5	6.5	6.75	6	5
Cure time (tc90, min)	18	15	16	15	14
Cure rate index (min ⁻¹)	9.5	11.8	10.8	11.1	11.1

CBS, *N*-cyclohexyl-2-benzothiazole sulfonamide.

aging accelerated for periods up to 7 days. Tensile strengths of the vulcanizates are plotted versus ageing time as shown in Figure 3. It is clear that tensile strength of the blank decreases dramatically, whereas tensile strength of NR/soda lignin composite decreases slightly upon ageing. On the other hand, NR/thiolignin composite shows the most thermally stable tensile strength with highest value after ageing for 7 days. Figure 4 illustrates that elongation at break of the blank vulcanizate decreases severely upon ageing. NR/soda lignin composite shows moderate change in elongation at break. However, NR/thiolignin possesses the best thermally stable elongation at break. Thus, elongation at break and tensile strength data are in agreement and both confirm thermal stability of NR/thiolignin composite.

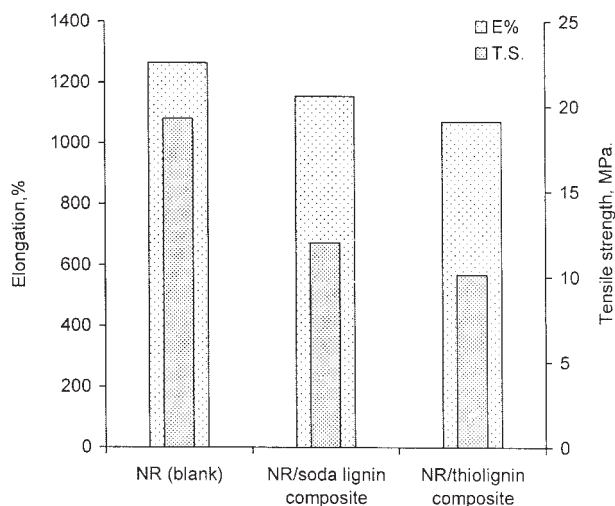


Figure 2 Tensile strength and elongation at break of NR and its composite vulcanizates.

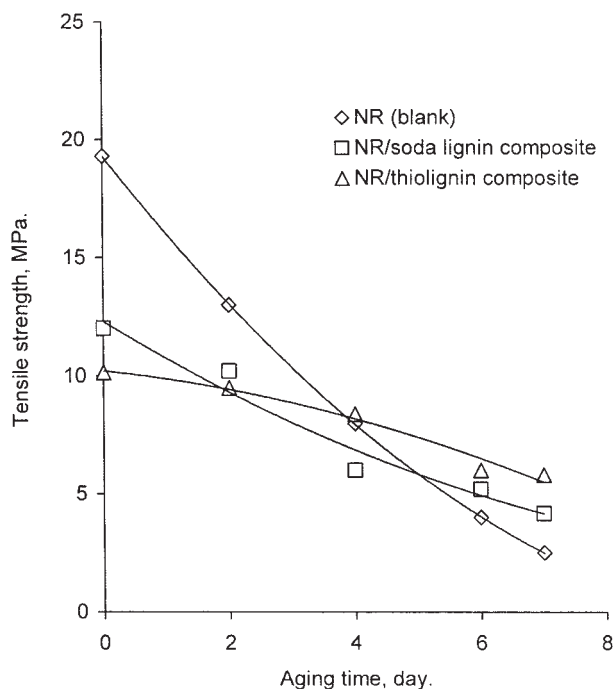


Figure 3 Tensile strength of NR and its composite vulcanizates vs. ageing time at 90°C.

NR/thiolignin composites with different thiolignin loadings

Thiolignin loading was then increased in its composite with NR to find whether there might be a certain thio-

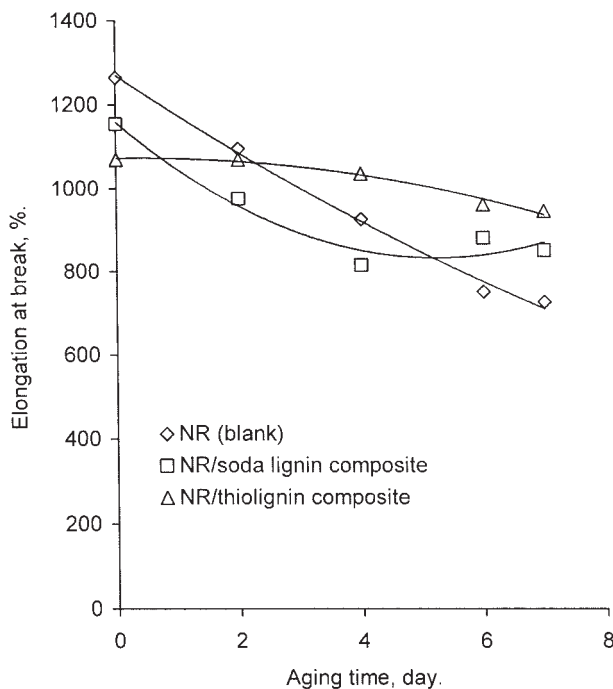


Figure 4 Elongation at break of NR and its composite vulcanizates vs. ageing time at 90°C.

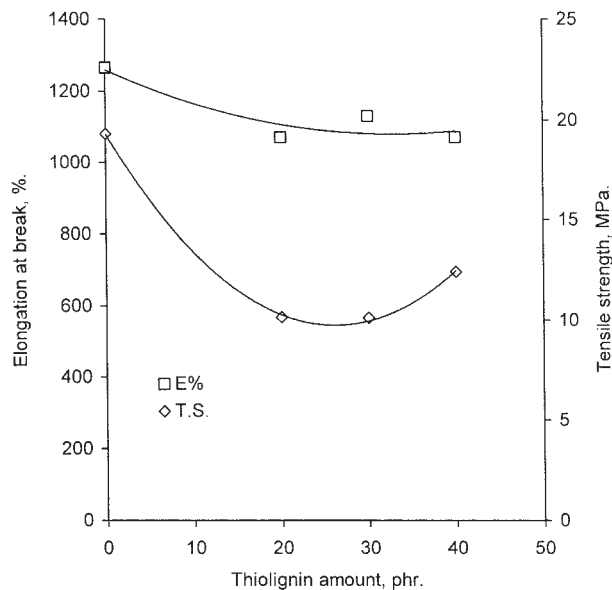


Figure 5 Tensile strength and elongation at break of NR composite vulcanizates vs. Thioliignin amount.

gnin loading that gives the most thermally stable composite. Formulations and rheological properties of the mixes are listed in Table II. It is obvious that further increase of thioliignin loading in the composite does not increase the maximum torque, but it results in a slight decrease in the cure time (t_{c90}). The physicomaterial properties of NR/thioliignin composites are plotted versus thioliignin amounts as shown in Figure 5. Elongation at break of the composite is not affected with the increase of thioliignin content in the composite. Also, a slight increase in tensile strength is noticed at 40 phr (parts per hundred parts rubber) thioliignin loading.

NR and NR/thioliignin composites with different amounts of thioliignin were then subjected to thermal ageing. It is obvious that tensile strength of the blank decreases with ageing time (Fig. 6). However, tensile strengths of the composites show less change upon ageing and the composite of thioliignin (20 phr) exhibits the best thermal stability. Elongation at break is plotted versus ageing time (Fig. 7). The composites with different amounts of thioliignin show less change in elongation at break than the blank. Thioliignin composite containing 20 phr thioliignin possesses the best thermally stable elongation at break.

Electric properties

Permittivity (ϵ') and dielectric loss (ϵ'') of the composites prepared were measured over the frequency range from 100 Hz to 100 kHz at temperature range from 20 to 80°C. The data obtained are illustrated graphically in Figure 8. It is clear that ϵ'' values decrease by increasing the applied frequency, showing an anomalous dispersion. In such range, the permittivity has

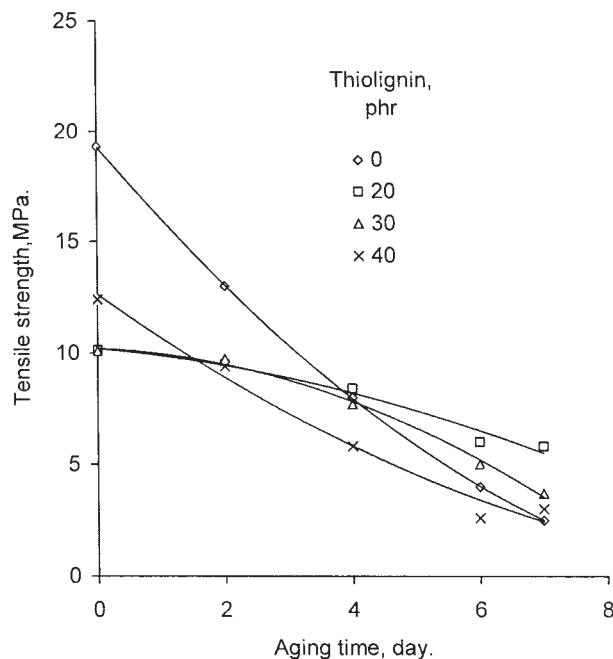


Figure 6 Tensile strength of NR vulcanizates with various thioliignin amounts vs. ageing time at 90°C.

contribution from orientation, atomic, and electronic polarization.²⁰ Also, it is clear that ϵ'' increases by increasing thioliignin content in NR/thioliignin composite. This can be attributed to the increase in the number of C=S dipoles, which leads to an increase in the orientation polarization.²¹ It is also apparent from Figure 8 that the value of ϵ'' increases by increasing

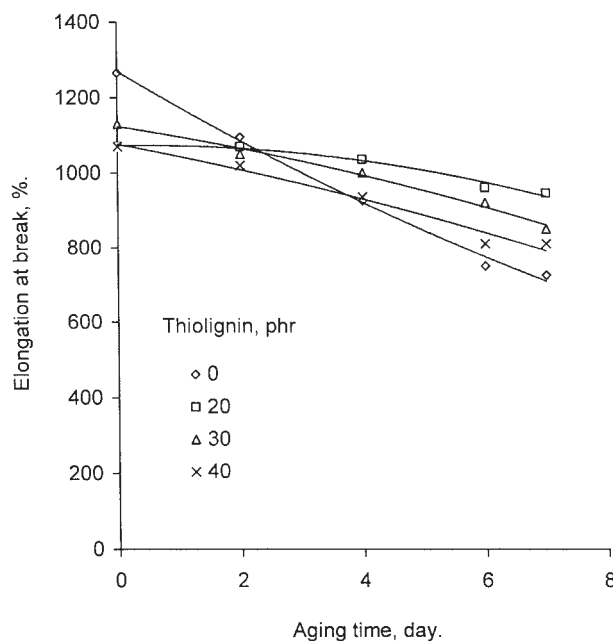


Figure 7 Elongation at break of NR vulcanizates with various thioliignin amounts vs. ageing time at 90°C.

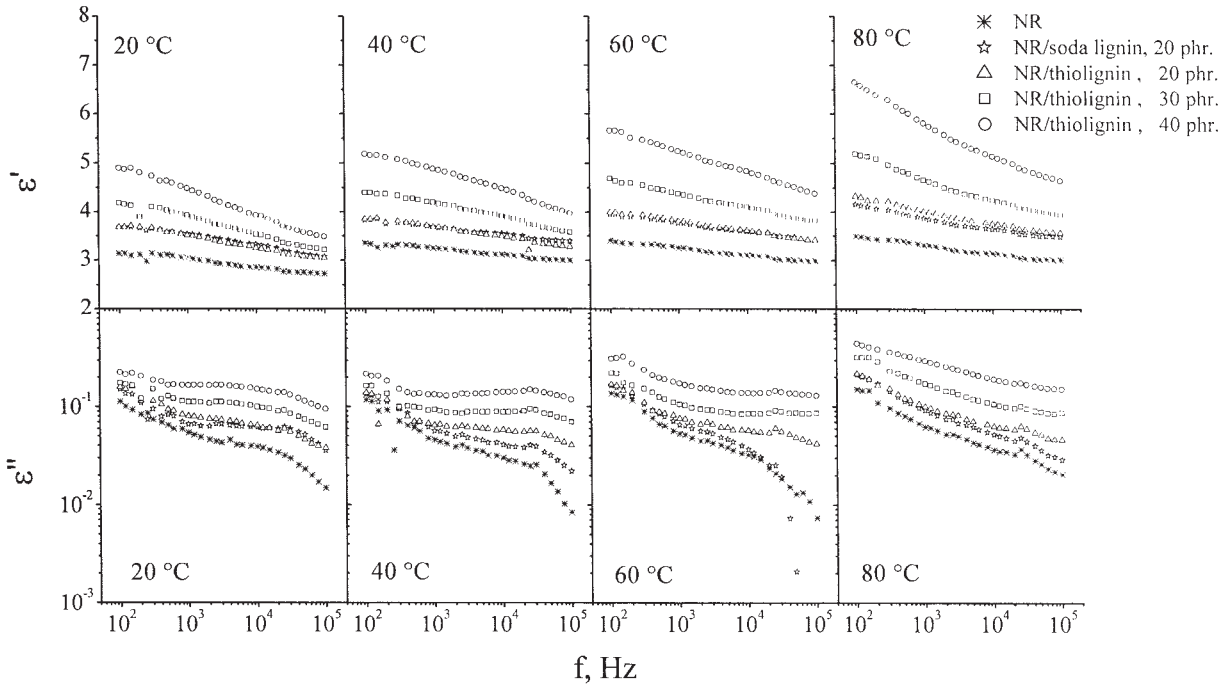


Figure 8 Permittivity ε' and dielectric loss ε'' vs. frequency (f).

temperature. From the same figure, it is clear that the curves relating ε'' and $\log f$ are broader than Debye curves,²² indicating that more than one relaxation process is present. It is also clear that ε'' increases slightly by increasing temperature. Fitting of the data was performed by a computer program based on all the different spectral functions commonly used in dielectric research, such as Debye,²³ Cole-Cole,²⁴ Cole-Davidson,²⁵ Havriliak-Negami,²² Fröhlich,²⁶ and Rocard-Powles.²² The best fitting of the data was done by a superposition of Havriliak-Negami and Fröhlich functions in addition to the conductivity term. On other words, the spectral function $\varepsilon''(\omega)$ could be expressed as:

$$\varepsilon''(\omega) = \varepsilon''(\omega)_{\text{HN}} + \varepsilon''(\omega)_{\text{Fr}} + \frac{\theta\sigma}{\omega}$$

The spectral function has been used to analytically represent the measured spectra. Where $\varepsilon''(\omega)_{\text{HN}}$ denotes Havriliak-Negami function form, $\varepsilon''(\omega)_{\text{Fr}}$ denotes Fröhlich function, ω is the angular frequency, σ is dc conductivity, and θ is a constant equals to $4\pi(9 \times 10^{11})$. Havriliak-Negami function is represented as:

$$\varepsilon''(\omega)_{\text{HN}} = \frac{(\varepsilon_s - \varepsilon_\infty)\sin\Phi\beta}{[1 + 2(\omega\tau_{\text{HN}})^{1-\alpha}\sin\pi\alpha/2 + (\omega\tau_{\text{HN}})^{2(1-\alpha)}]^{1/\beta}}$$

where

$$\Phi = \arctan \frac{(\omega\tau_{\text{HN}})^{1-\alpha}\cos\pi\alpha/2}{1 + (\omega\tau_{\text{HN}})^{1-\alpha}\sin\pi\alpha/2}$$

Also, α and β are Havriliak-Negami distribution parameters and ε_s and ε_∞ are the static permittivity and the permittivity at infinite frequency, respectively. While Fröhlich function is represented as:

$$\varepsilon''(\omega)_{\text{Fr}} = \frac{\varepsilon_s - \varepsilon_\infty}{P} \arctan \left[\frac{\sinh P/2}{\cosh \ln(\omega\bar{\tau}_{\text{Fr}})} \right]$$

P is a parameter describing width of the distribution of relaxation times between two limiting values τ_1 and τ_2 (where $P = \ln(\tau_1/\tau_2)$). $\bar{\tau}_{\text{Fr}}$ is the mean relaxation time and equals $(\tau_1\tau_2)^{1/2}$.

Examples of the dielectric spectrum and the fitting of the data for NR and NR/thiolignin (20 phr) at 20°C are illustrated graphically in Figure 9. Relaxation parameters obtained according to that fitting are given in Table III. The Havriliak-Negami distribution parameters α and β are equal to 0.2 and 0.56, respectively, for this fitting. Also, the width of the distribution of relaxation times P is varied from 3 to 4. The first absorption region, which lies approximately at $f \approx 0.175$ kHz, is found to be present for all the samples investigated. Those low-frequency losses may be attributed to Maxwell-Wagner losses arising from the interfacial polarization caused by the multi constituents of the investigated systems. The difference in permittivities and conductivities in the constituents of the investigated materials (see Table II) is considered to be the reason for the presence of such effect.

The second absorption region, which may be due to the aggregates¹⁵ expected to be formed by the addi-

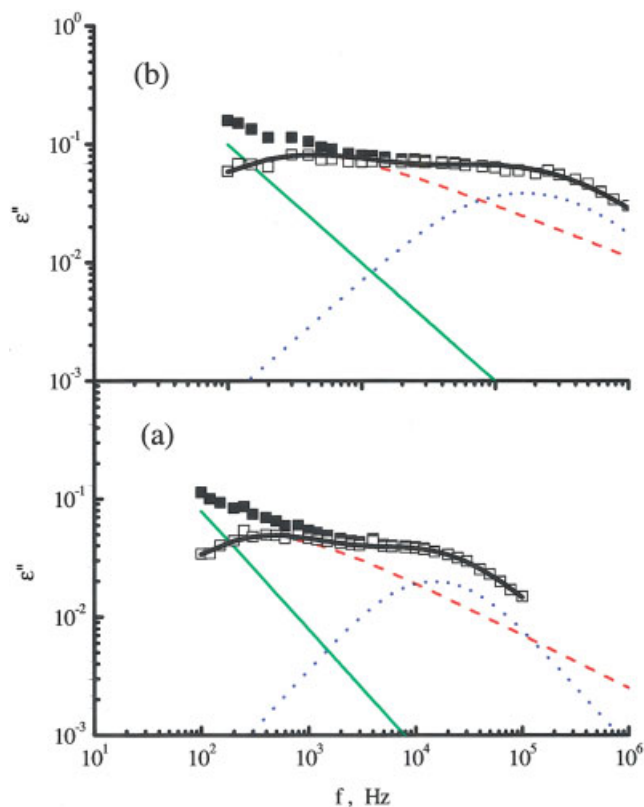


Figure 9 The absorption curve of (a) NR and (b) NR/thiolignin (20 phr) at 20°C. The data fitted by Havriliak-Negami and Fröhlich functions in addition to the conductivity term. (■) experimental data, (---) Havriliak-Negami, (—) ac conductivity, (□) dielectric loss after subtraction of conductivity, (····) Fröhlich, (— · —) total fit. [Color figure can be viewed in the online issue, which is available at www.interscience.wiley.com.]

tion of different ingredients to NR, is found to decrease slightly by the addition of either soda lignin or thiolignin to the NR (as seen from Table III). This result is comparable with that found before by other authors.^{27,28} The broadening (P varied from 3 to 4) of this absorption region with the increase of thiolignin content may be due to the fact that the micro-Brownian motions are controlled in part by the available free volume, a broader absorption curve could correspond to a broadened distribution of the free volume of the system.^{27,29} Also, by increasing the temperature, the relaxation time decreases. It seems to be interesting to study the activation energy E_A , which is defined as the energy sufficient to overcome the energy barrier separating the two mean equilibrium positions. Rate dynamic constant (R_{dc}) is temperature dependent. The dependency being related to the activation energy of this process is given by Arrhenius equation:

$$R_{dc} = A \exp(-E_A/kT)$$

Where R_{dc} is the rate dynamic constant (rate of dynamic process), A is a constant (the pre-exponential factor), k is Boltzmann's constant, and T is the absolute temperature. The activation energies, which were calculated from the second relaxation time E_{A_2} , increase from 7.50 to 17.17 J/mol by increasing the thiolignin loading. While in the case of soda lignin, the activation energy is about 4.10 J/mol. On the other hand, the change of the dc conductivity (σ) with the thiolignin content at different temperatures is shown in Figure 10. It is evident from that Figure that σ increases with increasing thiolignin content in NR/thiolignin composite. At low thiolignin loading, the conductivity increases slightly till the percolation threshold³⁰ (≈ 20 phr) beyond which the conductivity

TABLE III
Relaxation Parameters of NR Filled by Soda Lignin and Thiolignin

Temperature (°C)	S1	S2	S3	S4	S5
τ_1 (10^4 s)					
20	7.205	10.921	7.885	7.604	7.604
40	7.604	10.732	7.673	7.700	7.644
60	7.105	10.897	7.599	7.604	7.625
80	7.105	10.923	7.604	7.848	7.588
τ_2 (10^5 s)					
20	2.021	0.8268	0.9618	0.8234	0.7385
40	1.699	0.7061	0.8235	0.5333	0.4614
60	1.410	0.6627	0.6871	0.3852	0.3098
80	1.183	0.6164	0.5945	0.2493	0.2237
σ (S/m)					
20	4.380E-12	5.063E-12	5.523E-12	6.513E-12	8.106E-12
40	5.443E-12	6.068E-12	6.954E-12	8.106E-12	1.083E-11
60	6.764E-12	7.013E-12	8.105E-12	9.369E-12	1.346E-11
80	7.818E-12	8.106E-12	9.369E-12	1.123E-11	1.672E-11

τ_1 is the Havriliak-Negami relaxation time.

τ_2 is the Fröhlich relaxation time.

σ is the conductivity.

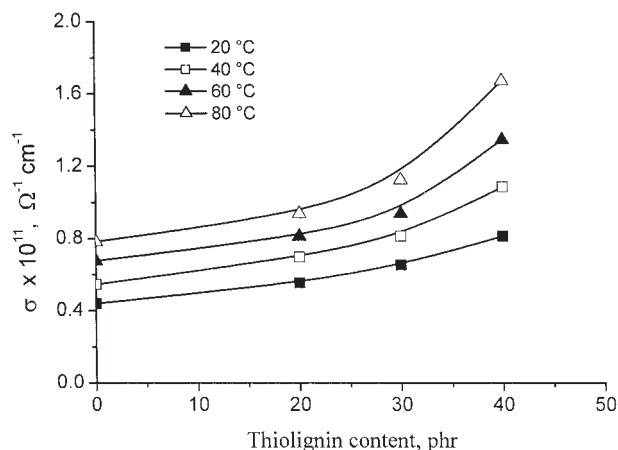


Figure 10 Conductivity (σ) vs. thiolignin content (phr) at different temperatures.

increases dramatically. This result is supported by the value of percolation threshold given using Janzen³¹ equation based upon the calculation of Zallen³² and Kirkpatrick³³ (even four samples were only used). Also, it is clear that the conductivity increases by increasing temperature.

CONCLUSIONS

1. Incorporation of either soda lignin or thiolignin into NR mixes results in composites with higher maximum torque and shorter cure time.
2. NR/soda lignin and NR/thiolignin composites possessed lower tensile strengths and slightly less elongations at break than the blank (NR) vulcanizate.
3. NR/thiolignin composite possessed the best thermal stability and the optimum thiolignin loading was found to be 20 phr.
4. Increasing the thiolignin loading in the NR/thiolignin composite resulted in the increase in ϵ' , which could be attributed to the increase in number of the C=S dipoles that leads to an increase in the orientation polarization.
5. Fitting of dielectric spectra of the composites under investigation reveals superposition of Havriliak-Negami and Fröhlich functions in addition to the conductivity term.
6. The first absorption region may be attributed to Maxwell-Wagner losses arising from the interfacial polarization caused by the multi constituents of the investigated systems.
7. The second absorption region may be attributed to the aggregates expected to be formed by the addition of different ingredients to NR.

8. The relation between dc conductivity and thiolignin content reveals that the percolation threshold was found to be ≈ 20 phr, indicating optimum thiolignin loading, which agrees with that obtained from thermal stability study.

References

1. Setua, D. K.; Shukla, M. K.; Nigam, V.; Singh, H.; Mathur, G. N. *Polym Compos* 2000, 21, 988.
2. Nagieb, Z. A.; Helaly, F. M.; Younan, A. F. *Res Ind* 1989, 34, 119.
3. Nitz, H.; Semke, H.; Mulhaupt, R.; Abacherli, A. *Kunststoffe/Plast Europe* 2001, 91(11), 98.
4. Faix, O. *Das Paperi* 1992, 12, 733.
5. Wu Shubin; Hu Yuan; Sun Liancao. *Cellulose Chem Technol* 1997, 31, 335.
6. Sundstrom, D.; Klei, H. E. *Biotechnol Bioeng Symp* 1982, 12, 45.
7. Martins, A. F.; Suarez, J. C. M.; Visconte, L. L. Y.; Nunes, R. C. R. *J Mater Sci* 2003, 38, 2415.
8. Martins, A. F.; Visconte, L. L. Y.; Nunes, R. C. R. *Kaut Gummi Kunstst* 2002, 55, 637.
9. Ismail, M. N.; Turky, G. M.; Nada, A. M. A. *Polym Plast Technol Eng* 2000, 39, 249.
10. Brezny, R.; Kovisikova, B. *Papira Celluloza* 1983, 25, 38.
11. Klimova, V. A.; Zapordina, K. S.; Zelinski, N. D. *Anal Khim* 1963, 18, 109.
12. ASTM designation, D 2084-95, 1998.
13. ASTM designation, D 412-98a, 1998.
14. ASTM designation, D 573-88, 1994.
15. Abd-El-Messieh, S. L.; El-Sabbagh, S.; Abadir, F. I. *J Appl Polym Sci* 1999, 73, 1509.
16. Seisto, A.; Poppius-Levlin, K. *TAPPI J* 1997, 80, 215.
17. Baeza, J.; Freer, J.; Pedreros, A.; Schmidt, E.; Mansilia, H.; Duran, N. *Don Bol Chil Quim* 1990, 35, 331.
18. Mansour, O. Y.; Nagaty, A.; Salama, M. A. *Paperi ja Puu* 1982, 64, 413, 417.
19. Bolker, H.; Somerville, N. G. *Pulp Pap Mag Canada* 1963, 64T, 187.
20. George, S.; Varughese, K. T.; Thomas, V. S. *J Appl Polym Sci* 1999, 73, 255.
21. Ku, C. C.; Liepins, R. *Electrical Properties of Polymers: Chemical Principles*; Hanser: Munich, Germany, 1987.
22. Mc-Crum, N. G.; Read, B. E.; Williams, G. *Anelastic and Dielectric Effects in Polymeric Solids*; Dover: New York, 1991.
23. Mantas, P. Q. *J Eur Ceram Soc* 1999, 19, 2079.
24. Stephanovich, V. A.; Glinchuk, M. D.; Hilczer, B. *Ferroelectrics* 2000, 240, 1495.
25. Blochowicz, T.; Tschirwitz, C.; Benkhof, S.; Rossler, E. A. *J Chem Phys* 2003, 118, 7544.
26. Abd-el-Messieh, S. L.; Mohamed, M. G.; Mazrouaa, A. M.; Soliman, A. *J Appl Polym Sci* 2002, 85, 271.
27. Ward, A. A. Ph.D. Thesis, Cairo University, Egypt, 2002.
28. Hakim, I. K.; Bishai, A. M.; Saad, A. L. *J Appl Polym Sci* 1988, 35, 1123.
29. Xu, J. W.; He, C. B.; Wei, T. S.; Chung, T. S. *Plast Rubber Compos* 2002, 31, 295.
30. Huang, J. C. *Adv Polym Technol* 2002, 21, 299.
31. Janzen, J. *J Appl Phys* 1975, 46, 966.
32. Zallen, R. *The Physics of Amorphous Solids*; Wiley: New York, 1983; Ch. 4.
33. Kirkpatrick, S. *Rev Mod Phys* 1973, 45, 574.